

Article

Structure and Magnetic Properties of a 1D Alternating Cu(II) Monomer—Paddlewheel Chain

Vanessa Machado ¹, Mark M. Turnbull ²  and Louise N. Dawe ^{1,*} 

¹ Department of Chemistry and Biochemistry, Wilfrid Laurier University, 75 University Ave. W., Waterloo, ON N2L 3C5, Canada; vmachado12@gmail.com

² Carlson School of Chemistry and Biochemistry, Clark University, 950 Main St., Worcester, MA 01610, USA; mturnbull@clarku.edu

* Correspondence: ldawe@wlu.ca; Tel.: +1-519-884-0710 (ext. 4963)

Received: 29 January 2018; Accepted: 26 February 2018; Published: 28 February 2018

Abstract: One-dimensional metal–organic coordination polymers make up a class of compounds with potential towards the development of practical, new magnetic materials. Herein, a rare example of an ABBABB coupled linear chain comprised of alternating dicopper(II) tetraacetate units bridged to copper(II) acetate monomer units *via* axial $\eta^2:\eta^1:\mu_2$ coordinated acetate is reported. Examination of the structure, determined by small molecule X-ray crystallography, shows that each Cu(II) ion is in a $d_{x^2-y^2}$ magnetic ground state. Magnetic susceptibility and magnetization data were collected and, consistent with the structural interpretation, demonstrate that the Cu(II) dimer (paddlewheel) exhibits classic antiferromagnetic exchange, while the $S = 1/2$ Cu(II) monomer is uncompensated in the ground state (low temperature regime.) Data were therefore fitted to a modified Bleaney-Bowers model, and results were consistent with the only other reported chain in this class for which magnetic data are available.

Keywords: copper(II) acetate; 1D-alternating chain; magnetic properties; X-ray structure

1. Introduction

Coordination polymers and metal–organic frameworks (MOFs) have been reported from a large variety of metal nodes and organic linker combinations, and range in size from micro [1,2]/nano [3] to mesoporous [4] materials. Leong and Vittal’s review [5] on 1D coordination polymers illustrates many examples reported from polydentate ligands with suitably disposed donor atoms for bridging two metals, but that still leave the metal coordination sphere unsaturated. As a result, further bonding to an additional donor ligand can take place, and result in an infinite repetition of one simple metal–organic building unit. Another recent review includes synthetic strategies for achieving alternating 1D coordination polymers *via* block-co-polymerization [6]. Further structural complexity and dimensionality for simple chains can be achieved through a variety of supramolecular means, including H-bonding [7–9], halogen bonding [10], and π -stacking [11].

These coordination polymers can have a variety of applications, and our interest is in the development of new magnetic materials. One technique to achieve magnetically active 1D coordination polymers is to include a magnetic sub-unit as a building block in the chain [5]. One subunit, for which exists a large body of literature, is the dicopper(II) tetracarboxylate-paddlewheel. Substitution at the axial water sites with ligands that possess multiple donor sites is amenable to the formation of 1D chains, which has led to a variety of bridged paddlewheel motifs. Percec and colleagues [12] performed a survey of the Cambridge Structural Database, and in 2010 reported three different motifs by which Cu(II) paddlewheels bridge themselves (without the requirement for any additional co-ligands) to generate 1D chains: an in-plane flat ribbon motif, and less commonly, two motifs of alternating in-plane and perpendicular bridging to adjacent carboxylates. Alternatively, the water could be replaced by

bridging heteroligands as reported, for example, for α -naphthoic acid [13] and 3-thiopheneacetate [14] paddlewheels with bridging 4,4'-bipyridine. These materials have a variety of uses, and one report has even demonstrated the potential use of pyridazine-bridged dicopper(II) tetracarboxylate 1D chains for gas adsorption [15].

Herein we report a new 1D coordination polymer consisting of alternating dicopper(II) tetraacetate units bridged to copper(II) acetate monomer units *via* axial $\eta^2:\eta^1:\mu_2$ coordinated acetate (Figure 1). The structural and magnetic properties of this uncommon repeating ABBABB motif are discussed.

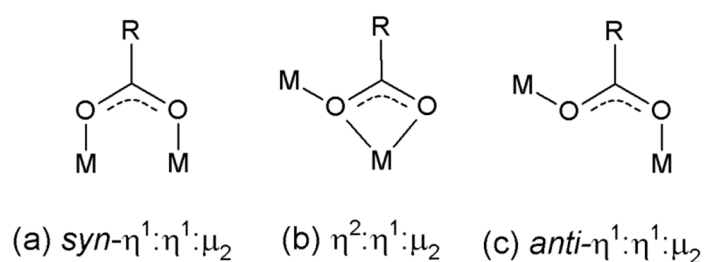


Figure 1. Selected coordination motifs for carboxylate-containing ligands.

2. Materials and Methods

2.1. Physical Measurements

Microanalyses were carried out by Midwest Microlab, Inc., Indianapolis, IN, USA. Infrared spectra were collected on a Perkin Elmer Spectrum BX, FT-IR System (Norwalk, CT, USA). Samples were prepared as KBr disks. Variable temperature magnetic data were obtained using a Quantum Design MPMS-XL SQUID magnetometer (San Diego, CA, USA). Background corrections for the sample holder assembly, measured independently, and diamagnetic components of the complexes were applied. Susceptibility data were taken over the temperature range from 1.8 to 310 K in an applied field of 1 kOe. Magnetization data as a function of applied field were collected from 0 to 50 kOe at 1.8 K. Several data points were collected as the field was returned to zero; no hysteresis was observed. Magnetic data were fitted using *MAGMUN4.1* software [16].

2.2. Synthesis

Catena-[hexakis(μ_2 -aceto)-bis(imidazole)tricopper(II)]; $\{\text{Cu}(\text{II})_3(\text{acetate})_6(\text{imidazole})_2\}_n$ (**1**): A clear, colorless solution of imidazole and 3,6-bis(imidazole-1-yl)pyridazine (0.121 g, 0.565 mmol) in methanol–acetonitrile (5 mL: 5 mL) was added dropwise to a solution of $\text{Cu}(\text{CH}_3\text{COO})_2 \cdot \text{H}_2\text{O}$ (0.226 g, 1.13 mmol) in methanol–acetonitrile (5 mL: 5 mL) forming a clear, light-blue solution that was stirred for twenty minutes with gentle heating ($\sim 60^\circ\text{C}$). This solution was then gravity filtered, and the filtrate kept for slow evaporation at room temperature. Blue crystals suitable for X-ray diffraction were collected after six weeks (0.140 g, 54.7 % yield). IR: 3121 cm^{-1} (m); 2931 cm^{-1} (m); 1637 cm^{-1} (m); 1560 cm^{-1} (s); 1459 cm^{-1} (s). Anal. calcd (%) for $\text{C}_{18}\text{H}_{26}\text{Cu}_3\text{N}_4\text{O}_{12} \cdot 0.5\text{H}_2\text{O}$: C, 31.33; H, 3.94; N, 8.12. Found (%): C, 31.28; H, 3.69; N, 8.06. The bulk crystalline sample was used for all analysis, and did not contain any 3,6-bis(imidazole-1-yl)pyridazine based on elemental analysis.

2.3. X-ray Crystallography

Data for a single crystal of **1**, measuring $0.233 \times 0.079 \times 0.54$ mm, were collected on a Bruker APEX-II CCD diffractometer (Madison, WI, USA). The crystal was kept at 110(2) K during data collection. SADABS-2014/5 [17] was used for absorption correction; $wR_2(\text{int})$ was 0.0634 before and 0.0489 after correction. Using Olex2 [18], the structure was solved with the ShelXT [19] structure solution program using direct methods and refined with the ShelXL [20] refinement package using least squares minimization. H-atoms were introduced in calculated positions and refined on a riding

model, except for H2, which was introduced in its difference map position, and refined positionally with a distance restraint. All non-hydrogen atoms were introduced in difference map positions and refined anisotropically.

Summary of crystal data for **1**: $C_{18}H_{26}Cu_3N_4O_{12}$ ($M = 681.05$ g/mol): monoclinic, space group $P2_1/c$ (no. 14), $a = 11.0485(17)$ Å, $b = 11.7850(17)$ Å, $c = 10.9549(16)$ Å, $\beta = 115.411(4)^\circ$, $V = 1288.4(3)$ Å³, $Z = 2$, $T = 110(2)$ K, $\mu(\text{CuK}\alpha) = 3.475$ mm⁻¹, $D_{\text{calc}} = 1.756$ g/cm³, 25574 reflections measured ($8.86^\circ \leq 2\theta \leq 133.232^\circ$), 2247 unique (2073 with $I > 2\sigma(I)$); $R_{\text{int}} = 0.0346$, $R_{\text{sigma}} = 0.0152$) which were used in all calculations. The final R_1 was 0.0240 ($I > 2\sigma(I)$) and wR_2 was 0.0637 (all data). Highest difference Fourier map peak 0.27 e/Å³ at $[0.7251, 0.1010, 0.7544]$, 0.74 Å from C5. CCDC1819987 contains the supplementary crystallographic data for this paper. These data can be obtained free of charge via <https://www.ccdc.cam.ac.uk/structures/> (or from the CCDC, 12 Union Road, Cambridge CB2 1EZ, UK; Fax: +44 1223 336033; E-mail: deposit@ccdc.cam.ac.uk.)

3. Results and Discussion

3.1. Structural Description

1 crystallized in the monoclinic space group $P2_1/c$. Cu1, and the symmetry related Cu1ⁱ ($i = 1-x, 1-y, 1-z$) define a dicopper(II) tetracarboxylate unit (Figure 2.) Cu1 is in a square pyramidal geometry, with four short contacts to O1, O2ⁱ, O3 and O4ⁱ, and one long contact to O5 (Table 1), defining the magnetic ground state as $d_{x^2-y^2}$. Cu2 is in a distorted octahedral environment, with two bidentate acetate ions, and two neutral *trans* monodentate imidazoles in its coordination sphere. It exhibits four short contacts to ligands which define the equatorial plane (Cu2-O6, Cu2-N1, and those related by symmetry; Table 1), and longer axial bonds to O5 and O5ⁱⁱ ($ii = 2-x, 1-y, 1-z$). The acetate ligand containing O5 therefore bridges the Cu1 dimer and the Cu2 monomer in an $\eta^2:\eta^1:\mu_2$ fashion (Figure 1), leading to an infinite one-dimensional chain parallel to the crystallographic *a*-axis (Figure 3). Further, the geometry about Cu2, with four “short” and two “long” bonds also defines a $d_{x^2-y^2}$ magnetic ground state, and the two “long”-bridged bonds (Cu1-O5 and Cu2-O5), with a large bond angle of $141.98(6)^\circ$, suggests poor magnetic orbital overlap between the monomer and dimer units (*vide infra*.) IR spectra are consistent with the presence of both acetate and imidazole ligands, with characteristic peaks for acetate observed at 2931 cm⁻¹ (alkyl C-H stretch) and 1637 cm⁻¹ (C=O stretch; shifted from 1605 cm⁻¹ in the IR of the starting material, copper(II) acetate hydrate), and for imidazole at 3121 cm⁻¹ (=C-H stretch) and 1560 cm⁻¹ (C=N stretch) (See Figure S1 in Supplementary Material).

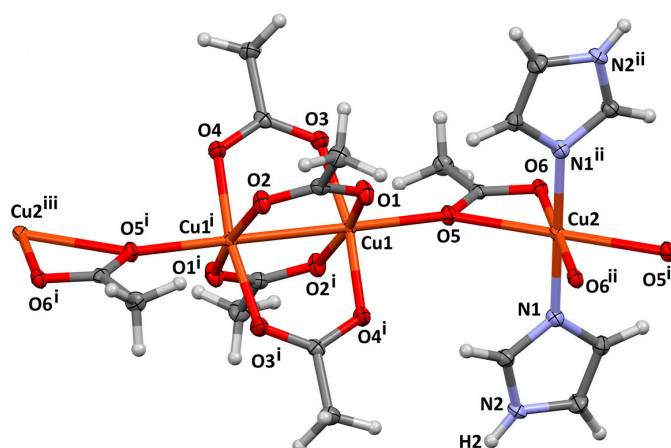
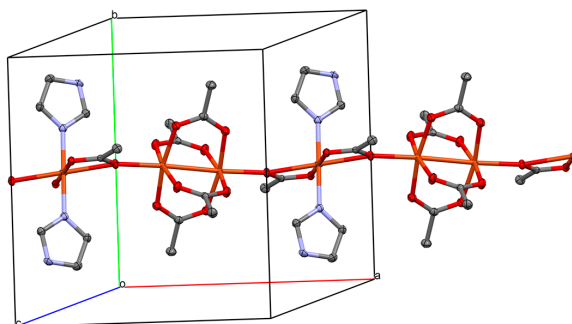


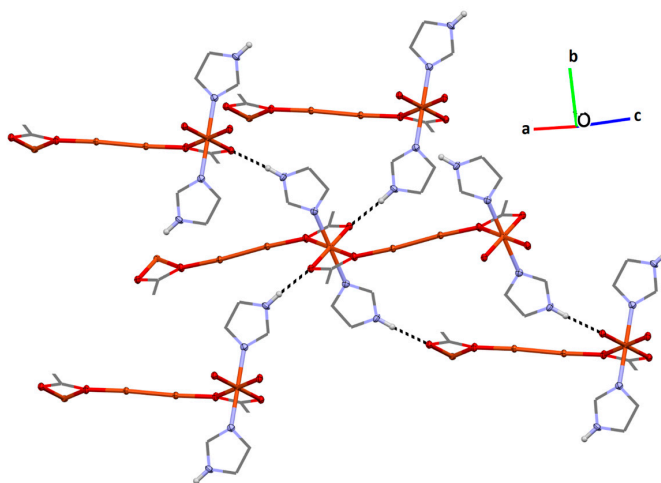
Figure 2. One subunit of the infinite chain for **1**, represented with 50% displacement ellipsoids. Symmetry codes: (i) $1-x, 1-y, 1-z$; (ii) $2-x, 1-y, 1-z$; (iii) $x-1, y, z$.

Table 1. Selected Bond Lengths (Å) and Angles (°).

Cu1-O1	1.9647(14)
Cu1-O2 ⁱ	1.9703(14)
Cu1-O3	1.9721(14)
Cu1-O4 ⁱ	1.9831(13)
Cu1-O5	2.1238(13)
Cu2-O5	2.4332(13)
Cu2-O5 ⁱⁱ	2.4332(13)
Cu2-O6	2.0352(13)
Cu2-O6 ⁱⁱ	2.0352(13)
Cu2-N1	1.9596(16)
Cu2-N1 ⁱⁱ	1.9596(16)
Cu1-O5-Cu2	141.98(6)

Symmetry codes: (i) $1-x, 1-y, 1-z$; (ii) $2-x, 1-y, 1-z$.**Figure 3.** Extended representation of **1** with 50% displacement ellipsoids; H-atoms omitted for clarity.

Interchain hydrogen bonding is observed between the Cu2-bonded donor imidazoles to one of the monomer acetate oxygen atoms ($\text{H2} \cdots \text{O6}$ 1.93(2) Å; $\text{N2-H2} \cdots \text{O6}$ 176(2)°; Figure 4.) The overall effect is that each Cu2 is involved in short outersphere interactions with four symmetry-related Cu2 moieties, each part of a different chain.

**Figure 4.** Interchain interactions for **1** via H-bonding (black dashed lines) from imidazole donors to the η^1 Cu2-bonded acetate oxygen atom. Paddlewheel acetates and H-atoms, except those on imidazole N2, have been omitted for clarity; 50% displacement ellipsoids, except carbon atoms, which are represented as wireframe.

This alternating Cu(II)-dimer \cdots Cu(II)-monomer carboxylate-bridged chain motif has been observed previously [21–23]. In the chain reported by Deka [21] and co-authors, acetate and imidazole are replaced by benzoate and 3,5-dimethylpyrazole, respectively. Therein, the Cu(II) monomer is very distorted from ideal octahedral geometry, owing at least in part to greater steric bulk from both ligands, and also from the ability of the protonated (uncoordinated) nitrogen of 3,5-dimethylpyrazole, to exhibit interchain hydrogen bonding with a dimer-coordinated benzoate oxygen-atom. The Cu(II)dimer-O_{benzoate}-Cu(II)monomer bond lengths and angles were 2.1733(17) Å, 2.684(2) Å and 131.28(8)°. Sarma [22] reports a near identical motif to Deka, again with 3,5-dimethylpyrazole, but with 4-methylbenzoate as the dimer and bridging monomer ligand. Cu(II)dimer-O_{benzoate}-Cu(II)monomer bond lengths and angles were 2.150(10) Å, 2.549(10) Å and 136.9(6)°. More recently, Zhang [23] has reported a structure with an acetate-based chain, however, in this case, each chain is bridged to two others *via* the axial monomer ligand, 2,6-di-imidazol-1-yl-pyridine, which coordinates at both terminal imidazole nitrogen sites. Cu(II)dimer-O_{acetate}-Cu(II)monomer bond lengths and angles were [2.170(3) Å, 2.665(4) Å and 131.81(17)°] and [2.165(3) Å, 2.744(4) Å and 130.86(16)°], for two distinct moieties in the crystallographic asymmetric unit. Note that while it is expected that each of these structures should exhibit antiferromagnetic coupling, dominated by the Cu(II) paddlewheel, with possible weak additional coupling *via* long axial bonds, or *via* the Cu_{dimer} \cdots O-C-O \cdots Cu_{monomer} η^1 : η^1 : μ_2 pathway, there has been no magnetic data previously reported.

3.2. Magnetic Studies

Magnetization as a function of field (Figure S2), and magnetic susceptibility as a function of temperature for **1** were measured and show a ground state of just less than one unpaired electron (saturation expected to be \sim 5700 emu/mol. It is possible that this may have been achieved if a field greater than 5 T had been available.) The magnetization data are consistent with a singlet ground state for the dicopper(II) tetracarboxylate moiety, with a residual spin from the Cu(II) monomer unit. A plot of χT vs. T (Figure 5; triangles) reveals that the high temperature χT limit was not yet achieved at 310 K, consistent with the presence of very strong exchange within the dicopper(II) tetracarboxylate moiety, and an essentially independent single Cu(II) ion. A plateau just over 0.4 (one Cu(II)) can be seen at low temperatures for χT vs. T, and then at the lowest temperatures a further drop is observed, possibly due to very weak interchain exchange *via* hydrogen bonding. Finally, the effect of the ‘uncoupled’ Cu(II) is enough to swamp the dimer at low temperature, so there is no maximum seen in the plot of χ vs. T (Figure 5, circles.)

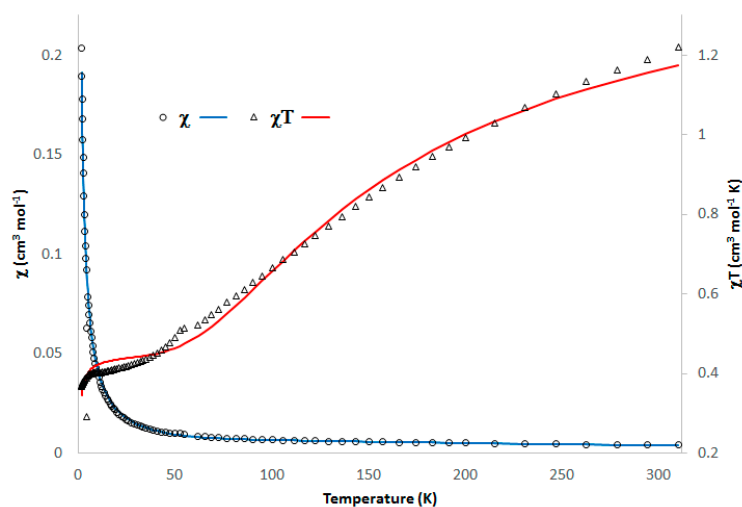


Figure 5. Magnetic susceptibility for **1**, expressed as χ vs. T (left, primary axis) and χT vs. T (right, secondary axis). Experimental data as circles (χ) and triangles (χT), and fitted model as solid lines.

The crystal structure indicates that **1** is a rare example of an ABBABB one-dimensional chain (Figure 6), which could be treated with two exchange values; J_d (exchange between the two copper(II) centers in the dimer; pathway A) and J_c (exchange between the dimer units and the monomer unit; pathway B.)

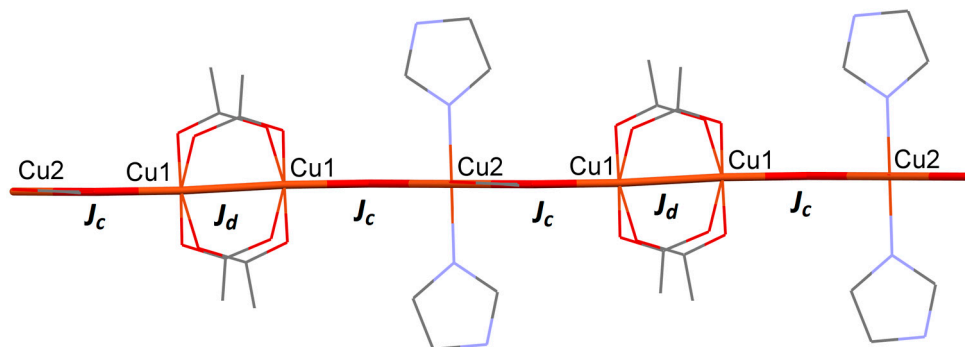


Figure 6. Wireframe and capped-stick representation of **1**, showing two possible superexchange pathways, with different coupling strengths (J_c and J_d).

Instead of fitting the data to a chain model, however, careful examination of **1** (*vide supra*) showed that each Cu(II) ion was in a $d_{x^2-y^2}$ magnetic ground state, with poor magnetic orbital overlap between the dimer and monomer units. This suggests that $J_c = 0$, and that the magnetic coupling can be described by the spin Hamiltonian:

$$H = -2JS_1S_2 \quad (1)$$

where $S_1 = S_2$ for Cu(II). The magnetism was therefore dominated by the paddlewheel coupling, and was fitted to a modified Bleaney–Bowers Equation (2):

$$\chi_M = \frac{2N_g^2\mu_B^2}{k(T-\theta)} \times \frac{1}{3 + e^{-\frac{2J_d}{kT}}} \times \rho + \frac{2N_g^2\mu_B^2}{4kT} + \frac{3N_g^2\mu_B^2}{4kT}(1-\rho) + N\alpha \quad (2)$$

where N is Avogadro's number, μ_B is the Bohr magneton, k is Boltzmann's constant, θ is a Weiss-like temperature correction, ρ a correction for any paramagnetic impurity, and $N\alpha$ is the temperature-independent paramagnetism. For **1**, $g = 2.17(1)$, $J_d = -190(6) \text{ cm}^{-1}$, $\theta = -0.5 \text{ K}$, $\rho = 0\%$, $N\alpha = 0.00028$ and $R = 4 \times 10^{-2}$ (solid lines in Figure 5.) The Weiss-correction is consistent with some weak interchain exchange. These results agree with the one previously reported Cu(II)-dimer...Cu(II)-monomer [24], where magnetic properties were studied (the ligand bridging the dimer and monomer units was tris(2-carboxyethyl) isocyanurate.) In that report Equation (2) was further modified to include a correction for interchain coupling (zJ'):

$$\chi = \frac{\chi_M}{1 - \left(\frac{2zJ'}{N_g^2\mu_B^2}\right)\chi_M} \quad (3)$$

to give $g = 2.19$, $J_d = -181.4 \text{ cm}^{-1}$, zJ' (interchain coupling) = -0.31 cm^{-1} , $\rho = 3.7\%$, $N\alpha = 0.00022$ and $R = 2 \times 10^{-5}$. The observed strong antiferromagnetic coupling for both reported ABBABB one-dimensional Cu(II) chains is the expected result of poor magnetic orbital overlap between A and B, and strong overlap between B (Cu(II) paddlewheels), *via* the four acetate bridges (with the exchange pathway between unpaired electrons in the Cu(II) $d_{x^2-y^2}$ orbitals, and the oxygen p_x -orbitals on acetate.) The classic example demonstrating strong antiferromagnetic coupling for isolated copper(II) acetate dimers was reported by Guha [25,26], and Bleaney and Blowers [27], originally in 1951 and 1952, respectively, and then re-examined by Elmali in 2000 [28], where $-2J$ was found to be 299.2 cm^{-1}

(i.e., $Jd = -150.6 \text{ cm}^{-1}$), with a Cu-Cu separation of 2.617(1) Å. This is comparable to the separation reported herein, of 2.5965(8) Å.

4. Conclusions

A new linear chain comprised of Cu(II) acetate dimer...Cu(II) acetate monomer units, assembled via the $\eta^2:\eta^1:\mu_2$ bonding of two acetate ligands has been reported. The magnetic properties are consistent with the assignment of $d_{x^2-y^2}$ magnetic ground states for each Cu(II) center. The Cu(II) dimer (paddlewheel) exhibits classic antiferromagnetic exchange, while the $S = 1/2$ Cu(II) monomer is uncompensated, and can be detected by both the remaining moment at low temperatures, as well as by the lack of a maximum in the magnetic susceptibility. Our future work in this area is focused on the possible applications of 1D chains in magnetic materials and for small molecule detection and uptake.

Supplementary Materials: The following are available online at <http://www.mdpi.com/2073-4352/8/3/114/s1>, Figure S1: IR of copper acetate and the reported Cu(II)-dimer... Cu(II)-monomer chain; Figure S2: Magnetization as a function of field for Cu(II)-dimer... Cu(II)-monomer chain; checkcif report for **1**.

Acknowledgments: Single crystal X-ray data for **1** was collected by Dr. Paul D. Boyle, Department of Chemistry X-Ray Facility, Western University, London, Ontario, Canada. VM would like to acknowledge support from the Faculty of Science Student Association, Wilfrid Laurier University. LND would like to thank Jason I. Mercer for very helpful discussions on fitting magnetic data. Funding support from Natural Sciences and Engineering Research Council of Canada, Canadian Foundation for Innovation, Wilfrid Laurier University Research Office, Dean of Science, and the Research Support Fund is acknowledged.

Author Contributions: Louise N. Dawe conceived and designed the experiments; Vanessa Machado performed the synthetic experiments; Mark M. Turnbull and Louise N. Dawe collected and analyzed the magnetic data; Louise N. Dawe analyzed all other data and wrote the paper.

Conflicts of Interest: The authors declare no conflict of interest.

References and Note

1. Xiang, S.; He, Y.; Zhang, Z.; Wu, H.; Zhou, W.; Krishna, R.; Chen, B. Microporous metal-organic framework with potential for carbon dioxide capture at ambient conditions. *Nat. Commun.* **2012**, *3*, 954. [[CrossRef](#)] [[PubMed](#)]
2. Zhang, Z.; Xiang, S.; Chen, B. Microporous metal-organic frameworks for acetylene storage and separation. *CrystEngComm* **2011**, *13*, 5983–5992. [[CrossRef](#)]
3. Yim, C.; Lee, M.; Yun, M.; Kim, G.-H.; Kim, K.T.; Jeon, S. CO₂-Selective nanoporous metal-organic framework microcantilevers. *Sci. Rep.* **2015**, *5*, 10674. [[CrossRef](#)] [[PubMed](#)]
4. Xuan, W.; Zhu, C.; Liu, Y.; Cui, Y. Mesoporous metal-organic framework materials. *Chem. Soc. Rev.* **2012**, *41*, 1677–1695. [[CrossRef](#)] [[PubMed](#)]
5. Leong, W.L.; Vittal, J.J. One-dimensional coordination polymers: complexity and diversity in structures, properties, and applications. *Chem. Rev.* **2011**, *111*, 688–764. [[CrossRef](#)] [[PubMed](#)]
6. Winter, A.; Schubert, U.S. Synthesis and characterization of metallo-supramolecular polymers. *Chem. Soc. Rev.* **2016**, *19*, 5311–5357. [[CrossRef](#)] [[PubMed](#)]
7. Zhang, W.X.; Shiga, T.; Miyasaka, H.; Yamashita, M. New approach for designing single-chain magnets: Organization of chains via hydrogen bonding between nucleobases. *J. Am. Chem. Soc.* **2012**, *134*, 6908–6911. [[CrossRef](#)] [[PubMed](#)]
8. Masu, H.; Tominaga, M.; Azumaya, I. Hydrogen-bonded 1D chains formed from adamantane-based bisphenols and bispyridines: Influences of substitution groups on phenol ring. *Cryst. Growth Des.* **2013**, *13*, 752–758. [[CrossRef](#)]
9. Wang, X.L.; Qin, C.; Wang, E.B. Polythreading of infinite 1D chains into different structural motifs: Two poly(pseudo-rotaxane) architectures constructed by concomitant coordinative and hydrogen bonds. *Cryst. Growth Des.* **2006**, *6*, 439–443. [[CrossRef](#)]
10. Shapiro, A.; Landee, C.P.; Turnbull, M.M.; Jornet, J.; Deumal, M.; Novoa, J.J.; Robb, M.A.; Lewis, W. Synthesis, structure, and magnetic properties of an antiferromagnetic spin-ladder complex: Bis(2,3-dimethylpyridinium) tetrabromocuprate. *J. Am. Chem. Soc.* **2007**, *129*, 952–959. [[CrossRef](#)] [[PubMed](#)]

11. Hu, K.-Q.; Zhu, L.-Z.; Wang, C.-Z.; Mei, L.; Liu, Y.-H.; Gao, Z.-Q.; Chai, Z.-F.; Shi, W.-Q. Novel uranyl coordination polymers based on quinoline-containing dicarboxylate by altering auxiliary ligands: From 1D chain to 3D framework. *Cryst. Growth Des.* **2016**, *16*, 4886–4896. [CrossRef]
12. Perec, M.; Bagglo, R.; Sartoris, R.P.; Santana, R.C.; Peña, O.; Calvo, R. Magnetism and structure in chains of copper dinuclear paddlewheel units. *Inorg. Chem.* **2010**, *49*, 695–703. [CrossRef] [PubMed]
13. Xu, W.; Zheng, Y.Q. One-dimensional polymers constructed with paddle-wheel dinuclear copper(II) bridged by 4,4'-bipyridine. *J. Chem. Crystallogr.* **2012**, *42*, 313–317. [CrossRef]
14. Marques, L.F.; Marinho, M.V.; Correa, C.C.; Speziali, N.L.; Diniz, R.; Machado, F.C. One-dimensional copper(II) coordination polymers based on carboxylate anions and rigid pyridyl-donor ligands. *Inorg. Chim. Acta* **2011**, *368*, 242–246. [CrossRef]
15. Takahashi, K.; Hoshino, N.; Takeda, T.; Noro, S.I.; Nakamura, T.; Takeda, S.; Akutagawa, T. Structural Flexibilities and Gas Adsorption Properties of One-Dimensional Copper(II) Polymers with Paddle-Wheel Units by Modification of Benzoate Ligands. *Inorg. Chem.* **2015**, *54*, 9423–9431. [CrossRef] [PubMed]
16. MAGMUN4.1: MAGMUN4.1/OW01.exe is available from the authors (<http://www.ucs.mun.ca/~lthomp/magmun/>). It was developed by Dr. Zhiqiang Xu and OW01.exe by Dr. O. Waldmann. Source codes are not distributed. The origin of the programs should be quoted.
17. SADABS; Bruker AXS Inc.: Madison, WI, USA, 2002.
18. Dolomanov, O.V.; Bourhis, L.J.; Gildea, R.J.; Howard, J.A.K.; Puschmann, H. OLEX2: A complete structure solution, refinement and analysis program. *J. Appl. Crystallogr.* **2009**, *42*, 339–341. [CrossRef]
19. Sheldrick, G.M. SHELXT—Integrated space-group and crystal-structure determination. *Acta Crystallogr. Sect. A Found. Crystallogr.* **2015**, *71*, 3–8. [CrossRef] [PubMed]
20. Sheldrick, G.M. Crystal structure refinement with SHELXL. *Acta Crystallogr. Sect. C Struct. Chem.* **2015**, *71*, 3–8. [CrossRef] [PubMed]
21. Deka, K.; Sarma, R.J.; Baruah, J.B. Nitrogen-oxygen bond formation during oxidative reactions of copper(II)benzoate complexes having 3,5-dimethylpyrazole. *Inorg. Chem. Commun.* **2006**, *9*, 931–934. [CrossRef]
22. Sarma, R.; Baruah, J.B. A mixed carboxylate polymer as an intermediate during synthesis of mononuclear bis-3, 5-dimethylpyrazole copper(II) benzoates. *J. Coord. Chem.* **2008**, *61*, 3329–3335. [CrossRef]
23. Zhang, J.; Zhang, C.; Yu, X.; Qin, Y.; Zhang, S. Two novel trinuclear cluster-based coordination polymers with 2,6-Di-imidazol-1-yl-pyridine: solvothermal syntheses, crystal structures, properties and Hirshfeld surface analysis. *Supramol. Chem.* **2016**, *28*, 231–238. [CrossRef]
24. Li, H.; Yao, H.; Zhang, E.; Jia, Y.; Hou, H.; Fan, Y. Crystal structures and magnetism of infinite alternating chains arranged by paddle-wheel dinuclear copper and mononuclear copper units. *Dalton Trans.* **2011**, *40*, 9388–9393. [CrossRef] [PubMed]
25. Guha, B.C. Magnetic properties of some paramagnetic crystals at low temperatures. *Proc. R. Soc. A* **1951**, *206*, 353. [CrossRef]
26. Guha, B.C. Magnetic properties of copper acetate at low temperatures. *Philos. Mag.* **1965**, *11*, 175–177. [CrossRef]
27. Bleaney, B.; Bowers, K.D. Anomalous paramagnetism of copper acetate. *Proc. R. Soc. A* **1952**, *214*, 451. [CrossRef]
28. Elmali, A. The magnetic super-exchange coupling in copper(II) acetate monohydrate and a redetermination of the crystal structure. *Turk. J. Phys.* **2000**, *24*, 667–672.

